

Comparative actualistic study hints at origins of alleged Miocene “coprolites” of Poland

Tomasz Brachaniec¹, Dorota Środek¹, Dawid Surmik¹, Robert Niedźwiedzki², Georgios L. Georgalis³, Bartosz J. Plachno⁴, Piotr Duda⁵, Alexander Lukeneder⁶, Przemysław Gorzelak⁷, Mariusz A. Salamon^{1*}

¹University of Silesia in Katowice, Faculty of Natural Sciences, Będzińska 60, 41-200 Sosnowiec, Poland, paleo.crinoids@poczta.fm (MAS - corresponding author)

²Institute of Geological Sciences, Wrocław University, Borna 9, 50-204 Wrocław, Poland

³Palaeontological Institute and Museum, University of Zurich, Karl Schmid-Strasse 4, 8006 Zurich, Switzerland

⁴Jagiellonian University in Kraków, Faculty of Biology, Institute of Botany, Gronostajowa Street 9, 30-387 Cracow, Poland

⁵University of Silesia in Katowice, Faculty of Science and Technology, Będzińska Street 39, 41-200 Sosnowiec, Poland

⁶Natural History Museum Vienna, Burgring 7, 1010 Vienna, Austria

⁷Institute of Paleobiology, Polish Academy of Sciences, Twarda 51/55, 00-818 Warszawa, Poland

Abstract

Excrement-shaped siderite masses have been the subject of much controversy. They have been variously interpreted either as being coprolites, cololithes or pseudofossils created by mechanical deformation of plastic sediment. Here we report excrement-shaped ferruginous masses recovered from the Miocene of Turów mine in south-western Poland.

Results of mineralogical, geochemical, petrographic and microtomographical analyses indicate that these masses consist of siderite and iron oxide rather than phosphate, and rarely contain recognizable food residues, which may suggest abiotic origins of these structures. On the other hand, evidence in support of a fecal origin include: (i) the presence of two distinct morphotypes differing in size and shape, (ii) the limited quantity of specimens, (iii) the presence of rare hair-like structures or coalified inclusions and (iv) the presence of rare fine striations on the surface. Importantly, comparative actualistic study of Recent vertebrate feces shows overall resemblance of the first morphotype (sausage-shaped with rare coalified debris) to excrements of testudinoid turtles (Testudinoidea), whose shell fragment was found in the investigated locality. The second morphotype (rounded to oval-shaped with hair-like

Comment [GM1]: Here and at some other places in the text, the format is “coprolites”. Elsewhere, the term is *coprolites*. I question the stylistic ethics of this format evolution, since the authors appear to be declaring the authenticity of the specimens before offering evidence to support this interpretation. For example, the material and methods declares the specimens to be coprolites long before and data is presented.

structures), in turn, is similar to the feces of some snakes (Serpentes), the remains of which were noted in the Miocene of the neighborhood areas.

Introduction

Incontrovertible examples of the Miocene coprolites are known from only a few localities in Europe, North and South America (Amstutz, 1958; Roberts, 1958; Hunt & Lucas, 2007, 2012, 2021; Dvořák et al., 2010; Godfrey & Smith, 2010; Hunt et al., 2012; Pesquero et al., 2014; Broughton, 2017; Dietzien-Dias, 2018; Tomassini et al., 2019; Farlow et al., 2020). Rodents, notoungulates, hathliacynid and borhyaenoid marsupials, indeterminate carnivorans, sirenians, crocodilians, were commonly invoked as potential producers of these coprolites (Godfrey & Smith, 2010; Dietzien-Dias, 2018; Tomassini et al., 2019). The majority of described Miocene vertebrate coprolites were produced by carnivores. This is not surprising because faeces of herbivorous tetrapods are commonly composed of a large quantity of undigested plant residues attracting microbial decomposition. On the other hand, the calcium phosphate derived from undigested bones in the faeces of carnivores acts as important permineralizing agent (e.g., Hunt et al., 1994; Pesquero et al., 2011; Dietzien-Dias, 2018). Excrement-shaped ferruginous masses have been considered (based on morphological grounds) by some authors as being coprolites (Amstutz, 1958; Broughton et al., 1977, 1978) or cololites (Seilacher et al., 2001; Broughton, 2017; intestinal casts - eviscerolites; see e.g., Hunt & Lucas, 2021). Notably, Broughton (2017) has recently described multi-decimetre-long intestine-like elongated objects revealing bilateral symmetry in cross-section and surface features consisting of fine longitudinal parallel striations, which were ascribed to gut casts of a previously unrecognized giant terrestrial earthworm.

Excrement-shaped masses are commonly reported from clay-rich sediments ranging in age from Permian to Holocene. However, given their ferruginous composition, significant variation in size, lack of internal inclusions, and scarcity of associated vertebrate remains, most authors rejected a zoological origin (Dake, 1939, 1960; Danner 1968, 1994, 1997; Major, 1939; Roberts, 1958; Spencer & Tuttle, 1980; Love & Boyd, 1991; Spencer, 1993, 1997; Hardie, 1994; Mustoe, 2001). Different non-zoological hypotheses have been invoked to explain the origins of these objects (such as soft sediment extrusion triggered by coseismic liquefaction (reference?), sediment intrusion into hollow logs (Spencer & Tuttle 1980, Spencer 1993) or squeezed between plant stems (Roberts 1958), expulsion of sediment in response to

Comment [GM2]: Incontrovertible? Amstutz (1958) described purported ferruginous coprolites from the Miocene Wilkes Formation in Washington State, USA, Roberts (1958) suggested the possibility that the objects were created when soft sediments were squeezed through plant stems. Later researchers (e.g., Danner, Spencer, Mustoe) all describe the specimens as being abiogenic. Seilacher (who only saw a few specimens that were purchased from a rock shop) described them as intestinal casts, a description that has been repeated by Broughton (another instance of an author who never visited the locality, and only examined a few specimens. After years of conflicting interpretations, it is certainly not correct to describe the 1958 report of Amstutz as incontrovertible.

Comment [GM3]: One of the most abundant occurrences of ferruginous "coprolites" is the Cretaceous White Mud Formation of Saskatchewan, Canada, a locality that deserves to be mentioned.

Comment [GM4]: Here's a story that relates to the Cretaceous White Mud Formation "coprolites" from Saskatchewan, Canada. In a 1977 and 1978 papers Broughton et al. declared that the trace makers were most likely big fish, e.g., sturgeon and bowfin. In 2014, Broughton proposed that the ferruginous masses included intestinal casts of a herbivorous reptilian tetrapod. In 2017, Broughton decided that these trace fossils were instead made by giant earthworms. This calls into question the wisdom of declaring reported coprolite occurrences as "incontrovertible".

Comment [GM5]: Doesn't this conflict with the valid comment that plant materials are susceptible to microbial decomposition? Earthworm guts presumably contain no calcium phosphate.

gravity (Love and Boyd 1991), and extrusion of siderite related to methanogenesis (Mustoe 2001).

Until recently, a detailed study on excrement-shaped ferruginous masses from the Miocene of Poland has been lacking. In this paper we analyse the Miocene excrement-shaped specimens collected from the coal mine of Turów for the first time. According to our results, we favour the hypothesis that the specimens from Poland may represent true coprolites and more particularly pertaining to two different reptile groups.

Geological setting

The Turów lignite mine is located in the south-eastern part of the Lower Silesia Voivodeship (SW Poland) and covers the former village of Turów. It is located in the central part of the Silesia region Żytawa-Zgorzelec Depression located between the state borders of Germany and the Czech Republic (Fig. 1A). Turów lignite deposits are part of the Upper Lusatian Brown Coal Basin. This basin comprises a few tectonic sinkholes (Piątkowska et al., 2000) that developed in Paleogene at the junction of two regional zones of strong activity: Ore Mts. Graben (Ohrza rift) and the Lusatian-Elbe Tectono-Volcanic Zone (Jęczmyk & Sztromwasser, 1998). The most southern of these is the Zittau basin (Fig. 1A, B), which was filled mainly by limno-fluvial or limnic clays, silts, sands and thick layers of lignites exploited in the Turów mine (Kasiński, 2000; Kasiński et al., 2015). Furthermore, there are numerous vulcanite rocks of late Eocene, Oligocene and early Miocene age (Kasiński et al., 2015). The basal part of sedimentary section of the Zittau basin is not older than the early Oligocene, however most sediments were formed in the Miocene (Kasiński et al., 2015). At the base of the Zittau Basin, Precambrian and Palaeozoic metamorphic and igneous rocks are present (Marcinkowski, 1985).

The lithological profile of the Turów mine is ca. 250 m thick and consists of 7 lithostratigraphic units of sedimentary rocks. Apart from the two youngest units (Gozdnica Fm. and glacial tills), all of them are mainly composed of clays and/or muds. Additionally, there are coal seams, especially in Opolno and Biedrzychowice formations, which are the deposits mined at the Turów mine. The oldest Cenozoic sediments of the profile are Oligocene sediments (Egger age), forming the lower part of the Turoszów Fm. (Kasiński et al., 2015). The youngest in the profile are Gozdnica Fm. and Pleistocene deposits, mainly represented by Pannonian tills (Marcinkowski, 1985).

Comment [GM6]: References should be cited for these hypotheses

Love, J.D. and Boyd, D.W., 1991. Pseudocoprolites in the Mowry Shale, (Upper Cretaceous), northwest Wyoming. University of Wyoming Contributions to Geology, v.28, 130-144.

Comment [GM7]: A stratigraphic section, even a generalized one, would be a great asset

101 The Turoszów Fm. was formed in fluvial and limnofluvial conditions, while the
102 Opolno and Biedrzychowice Fms have been formed in limnotelmatic environments, and
103 Porajów Fm. represents limnofluvial environment. Sediments of the upper part of Miocene
104 profile (Rybarzowice and Gozdnicza Fms) have alluvial origin (Kasiński et al., 2003).

105 Biedrzychowice Fm., within which excrement-shaped ferruginous masses and a turtle remain
106 have been documented, was formed in vast swamps and rushmarshes (Kasiński et al., 2010).

107 Especially in the upper part of this formation, there are numerous palaeosols levels with plant
108 roots and trunks preserved in situ (Kasiński & Wiśniewski, 2003). Marsh forests mainly
109 composed of *Cupressaceae* and *Taxaceae* (Sadowska, 1995; Kasiński & Wiśniewski, 2003).

110 Based on palaeobotanical analysis of the coal seam it was concluded that there was a humid
111 warm temperate climate similar to that of south-eastern China today (Durska, 2008; Kasiński
112 et al., 2010). The excrement-shaped ferruginous masses and the turtle shell fragment

113 documented in this article were collected in an inactive part of the excavation, within the clays
114 of the higher part of Biedrzychowice Fm. in the uppermost part of early Miocene

115 (Burdigalian; see Fig. 1C). Two distinct morphotypes randomly distributed within clay and
116 mudstone on the flat surface of the excavation were noted.

117

118 Figure 1 around here

119

120 Fossil content in the Turów area and adjacent areas

121

122 No animal fossil remains have been documented so far from the Oligocene–Miocene of the
123 Zittau Basin with exception of burrows of sediment eating fauna (Kasiński et al., 2015). In the
124 course of the present research in the clays of Biedrzychowice Fm, apart from the excrement-
125 shaped ferruginous masses, a fragment of a turtle shell was found. This shell fragment (see
126 Fig. 3N) can only be identified as an indeterminate testudinoid. This turtle lineage is
127 otherwise abundant in Oligocene and early Miocene localities in Germany and Czech
128 Republic (Reinach, 1900; Młynarski & Roček, 1985), but had not so far been documented
129 from coeval localities in Poland. In older, Eocene and Oligocene localities in the neighbouring
130 north-western Czech Republic and south-eastern Germany (Saxony and southeastern Saxony-
131 Anhalt), rich assemblages of terrestrial-aquatic tetrapod fauna have been documented,
132 comprising frogs, salamanders, choristoderans, crocodiles (also crocodile coprolites, see
133 Kasiński et al., 2015, and literature cited therein), turtles, lizards, and snakes (Table 1).

134

Comment [GM8]: This can hardly be considered a terrestrial environment. Note that the “coprolites” are reported to have come from clay beds, not coal seams. As I note later, the decision to consider only excrements from modern terrestrial animals does not match the taphonomy.

Formatted: Highlight

Formatted: Highlight

Comment [GM9]: A problem here is that discovery of fossils provides important information about the presence of ancient life forms, but there may be many other creatures whose fossilized remains have not yet been found. “Absence of evidence is not proof of absence”

135 **Table 1.** Oligocene vertebrates (amphibians and reptiles) collected in adjacent areas (north-
136 western Czech Republic and south-eastern Germany [Saxony, south-eastern Saxony-Anhalt]);
137 after Laube, 1901; Obrhelová, 1971; Špinar, 1972; Obrhelová & Obrhel, 1987; Szyndlar,
138 1994; Böhme, 1996, 1998, 2007; Gaudant, 1996, 1997; Micklich & Böhme, 1997; Bellon et
139 al., 1998; Kvaček & Walther, 2003; Mikuláš et al., 2003; Fejfar & Kaiser, 2005; Karl, 2007;
140 Čerňanský & Augé, 2012, 2013; Čerňanský et al., 2016; Georgalis & Joyce, 2017; Chroust et
141 al., 2019.

142

Age	Locality	Amphibians	Reptiles
late Oligocene	Lužice-Žichov (Czech Republic)	<i>Triturus opalinus</i> <i>Rana luschnitzana</i> <i>Asphaerion reussi</i>	
	Sulečice (Czech Republic)	<i>Archaeotriton basalticus</i> <i>Palaeobatrachus grandipes</i> <i>Palaeobatrachus laubei</i>	
	Bechlejovice (Czech Republic)	<i>Archaeotriton basalticus</i> <i>Palaeobatrachus diluvianus</i> <i>Palaeobatrachus luedeckei</i> <i>Palaeobatrachus robustus</i> <i>Palaeobatrachus grandipes</i> <i>Palaeobatrachus novotnyi</i> <i>Eopelobates bayeri</i>	' <i>Diplocynodon</i> ' sp.
early Oligocene	Espenhain, Saxony (Germany)		Trionychidae indet. <i>Peloroichelon</i> sp. <i>Diplocynodon</i> sp.
	Kundratice (Czech Republic)	<i>Palaeobatrachus</i> sp. cf. <i>Eopelobates</i> sp.	cf. <i>Diplocynodon</i> sp.
	Lukavice (Czech Republic)		' <i>Diplocynodon</i> ' sp.
	Markvartice (Czech Republic)	<i>Chelotriton laticeps</i> <i>Palaeobatrachus diluvianus</i> <i>Palaeobatrachus luedeckei</i> <i>Palaeobatrachus</i> sp.	
	Dětaň (Czech Republic)	Salamandridae indet. Palaeobatrachidae indet. Pelobatidae indet.	Lacertidae indet. Anguidae indet. Testudinidae indet.

		Discoglossidae indet.	Serpentes indet. Crocodylia indet.
--	--	-----------------------	---------------------------------------

143

144

145

146

147

148

149

150

151

152

153

154

155

156

From the other hand, in the lower Miocene clays and sands of North Bohemian Brown Coal Basin, a very rich fauna assemblage was reported (Klembara, 1979, 1981; Roček, 1984; Szyndlar, 1991a, b; Szyndlar & Schleich, 1993; Szyndlar & Rage, 2003; Čerňanský, 2010a, b; Dvořák et al., 2010). The latter mentioned and illustrated numerous invertebrate sand vertebrates represented by osteichthyan fish, amphibians, reptiles, birds, and mammals. The reptile taxa are shown in the table below (Table 2).

Table 2. Reptiles recorded in the lower Miocene deposits of North Bohemia, Czech Republic (taken from Klembara, 1981, 2008, 2012, 2015; Młynarski et al., 1985; Ivanow, 2002; Čerňanský & Joniak, 2009; Čerňanský, 2010, 2012; Čerňanský & Bauer, 2010; Čerňanský et al., 2015; Dvořák et al., 2010; Joyce, 2016; Georgalis & Joyce, 2017; Klembara & Rummel, 2018; Chroust et al., 2021).

turtles	crocodiles	lizards	snakes	choristoderans
			Scolecophidia indet.	
			<i>Bavarioboa hermi</i>	
	<i>Diplocynodon</i> cf. <i>ratelii</i>	<i>Merkurosaurus</i> <i>ornatus</i>	<i>Bavarioboa</i> sp.	<i>Lazarussuchus</i> <i>dvoraki</i>
			Constrictores indet.	
			<i>Falseryx</i> <i>petersbuchi</i>	
		<i>Pseudopus</i> <i>ahnikoviensis</i>	“ <i>Coluber</i> ” <i>dolnicensis</i>	
		<i>Pseudopus confertus</i>	<i>Texasophis</i> <i>bohemicus</i>	
		<i>Pseudopus</i> sp.		
		<i>Ophisaurus fejfari</i>		
<i>Rafetus bohemicus</i>		<i>Ophisaurus holeci</i>	“ <i>Coluber</i> ” <i>suevicus</i>	
		<i>Ophisaurus robustus</i>		
		<i>Ophisaurus spinari</i>		
		<i>Ophisaurus</i> aff. <i>spinari</i>		
		<i>Ophisaurus</i> sp. (two		

		morphotypes)		
		Anguinae indet. (several morphotypes)		
		<i>Palaeocordylus bohemicus</i>		
Trionychinae indet.		aff. <i>Palaeocordylus bohemicus</i>	“ <i>Coluber</i> ” <i>caspioides</i>	
			“Colubrinae” indet.	
<i>Ptychogaster laubei</i>		<i>Euleptes gallica</i>	<i>Elaphe</i> sp.	
<i>Ptychogaster</i> cf. <i>emydoides</i>		<i>Chamaeleo andrusovi</i>		
<i>Ptychogaster</i> sp.		Chamaeleonidae indet.	<i>Natrix sansaniensis</i>	
		<i>Amblyolacerta dolnicensis</i>		
<i>Chelydropsis</i> sp.		<i>Lacerta</i> sp.	<i>Natrix merkurensis</i>	
		<i>Miolacerta tenuis</i>	<i>Neonatrix nova</i>	
		Lacertidae indet.	<i>Palaeonatrix lehmani</i>	
		cf. Scincidae indet.		
		<i>Blanus gracilis</i>	Natricinae indet.	
		Squamata indet.	Elapidae indet.	
			<i>Macrovipera platyspondyla</i>	
			<i>Vipera antiqua</i>	
Testudinidae indet.			<i>Vipera</i> sp.	
			Viperidae indet.	

157

158 Material and methods

159

160 Among 29 coprolites obtained from the investigated locality, 10 representative coprolites
161 were selected for detailed investigation. A tortoise shell fragment, documented
162 macroscopically in the field and found on a flat surface of upper part of the Biedrzychowice
163 Fm., was also subjected to further observations. All specimens are housed in the Institute of
164 Earth Sciences of the University of Silesia in Katowice, Poland, and catalogued under
165 registration number GIUS 10-3739.

166 A clay sample weighing ca. 40 kg was also collected from Biedrzychowice Fm. and
167 transported to the Laboratory of the Institute of Earth Sciences of the University of Silesia in
168 Katowice. It was washed using running hot tap water, screened on a sieve column ($\varnothing 1.0$,
169 0.315 and 0.1 mm-mesh respectively), and finally dried at 180°C. This washed and dried
170 residue was observed under a Leica WildM10 microscope for vertebrate remains;
171 unfortunately, nothing was found in the residue.

172 Coprolites recorded herein have been investigated with a number of different
173 analytical tools.

174

175 *Optical microscopy*

176

177 Optical observation of thin sections were carried out using Leica SZ-630T dissecting
178 microscope and Nikon Eclipse E100 light microscopy, while the microphotographs were
179 collected using Olympus BX51 polarizing microscope equipped with an Olympus SC30
180 camera and a halogen light source, installed Faculty of Natural Sciences at the University of
181 Silesia in Katowice (Poland).

182

183 *Scanning Electron Microscopy*

184

185 The chemical composition, morphology of coprolite matrix and microstructures topography
186 were investigated using the desktop scanning electron microscopy (SEM) Phenom XL,
187 Phenom World (Thermo Fisher Scientific, Eindhoven, Netherlands) equipped with a fully
188 integrated energy-dispersive X-ray spectroscopy (EDS) detector and secondary electron
189 detector (SED) located in the Faculty of Natural Sciences at the University of Silesia in
190 Katowice (Poland). Measurements were performed with low-vacuum settings with
191 accelerating voltage 15kV.

192

193 *Microtomography*

194

195 Virtual sections of a selected specimen (GIUS 10-3739/23) were made in the Faculty X-ray
196 Microtomography Laboratory at Faculty of Computer Science and Material Science,
197 University of Silesia in Katowice, Chorzów, Poland using the General Electric Phoenix
198 v|tome|x micro-CT equipment at 160 kV, 70 μ A and scanning time of 20 min. Projection
199 images were captured using a 1000 \times 2024 ppx scintillator/CCD with an exposure time of 250

ms and processed using Volume Graphics® VGSTUDIO Max software and analysed using Volume Graphics® myVGL viewer.

Thin-sectioning

Thin sections from two specimens representing two morphotypes were made in the Grindery at the Faculty of Natural Sciences, University of Silesia in Katowice, Sosnowiec, Poland. Specimens were embedded in Araldite epoxy resin, sectioned, mounted on the microscope slides and polished with silicon carbide and aluminium oxide powders to about 30 µm thick.

Confocal Raman spectroscopy

To determine the mineralogical composition, the WITec confocal Raman microscope CRM alpha 300M equipped with an air-cooled solid state laser ($\lambda = 532$ nm and $\lambda = 457$ nm) and an electron multiplying CCD (EMCCD) detector was used. The calibration of the instrument was verified by checking the Si position. The Raman scattered light was focused onto a multi-mode fiber and monochromator with a 600 line/mm grating. To collect spectra of the coprolite matrix phases, the 50x/0.76NA and 100x/0.9NA air Olympus MPLAN objectives were used. All spectra were collected in the 200-4000 cm^{-1} range with 3 cm^{-1} spectral resolution. A surface Raman imaging map was collected in a 140 x 25 µm area using 140 x 20 pixels with an integration time of 0.5 s per spectrum, and precision of moving the sample during the measurements of ± 0.5 µm. The cluster analysis was performed to group spectra into clusters. K-means analysis with the Manhattan distance for Raman imaging maps was carried out. The data obtained was manipulated by WITec Project FIVE Software (cosmic rays removal procedure and cluster analysis) and GRAMS software package (baseline correction).

XRD

Bulk mineral composition of two powdered specimens representing each morphotypes was determined by Debye-Sherrer X-ray method using Rigaku SmartLab diffractometer equipped with Cu K α 1 source radiation. Measurement parameters were: acceleration voltage: 45 kV; filament current: 200 mA; step size: 0.05° 2 θ . Analyses of the collected data were carried out by means of XRAYAN Software using the newest ICSD database.

234 *Observations of extant excrements*

235

236 Faeces of Recent animals (private farms and from animals raised at the Silesian Zoological
237 Garden in Chorzów, Poland) were observed. Over the course of two months, a total of 787
238 excrements belonging to modern fish, amphibians, reptiles, birds and mammals were
239 collected. Lineages that had their representatives in the early Miocene sediments of North
240 Bohemia, Czech Republic (see Tables 3-6) were selected for a more detailed observation.
241 Additionally, the animals had to be large enough to produce excrements with dimensions
242 comparable to those currently documented in the fossil state. Thus, the faeces of small fish,
243 the remains of which are known from the Miocene sediments of North Bohemia, such as
244 *Chalcaburnus* or *Nemacheilus*, toads and frogs (*Rana*, *Pelobates*), birds (*Upupa*, *Coturnix*)
245 and mammals (*Chiroptera*, *Dryomys*, *Sciurus*, *Martes*), were not taken into account.

246 Those taxa that left their excrement in the aquatic environment were also rejected; the
247 exception was fish. The same remark applies to crocodile and some lizard excrements, which,
248 based on the observations in the Silesian Zoological Garden, left their faeces in the aquatic
249 environment. Only those that left at least part of their faeces in the terrestrial environment
250 were selected for subsequent observations. These were snakes [the king python
251 (*Pythonregius*), the tiger python (*Pythonmolurus*), the reticulated python (*Malayopython*
252 *reticulatus*), the common boa (*Boa constrictor*), the king cobra (*Ophiophagus hannah*), the
253 Korean rat snake (*Elaphe anomala*), the common European viper (*Vipera berus*)], lizards [the
254 komodo dragon (*Varanus komodoensis*)], and turtles [the Mediterranean tortoise (*Testudo*
255 *hermanni*), the steppe tortoise (*Testudo horsfieldii*), the Indian star tortoise (*Geochelone*
256 *elegans*), the Spanish pond turtle (*Mauremys leprosa*), and the Nile soft shell turtle (*Trionyx*
257 *triunguis*)].

258

259 **Table 3.** List of taxa of observed fish excrements. Fossil representatives taken from Hunt &
260 Lucas, 2007.

261

modern fish	fossil representative
<i>Aspius</i> sp.	<i>Aspius</i> sp., <i>Aspius laubei</i> , <i>Barbus</i> sp., <i>Barbus bohemicus</i>
<i>Leuciscus</i> sp.	<i>Palaeoleuciscus</i> sp., <i>Palaeoleuciscus chartacerus</i>

Comment [GM10]: This is a doubtful argument, because the sediments that contain the coprolites were deposited in fluvial or lacustrine environments. Except for tortoises, most turtles dwell in aquatic habitats. Very few snakes are aquatic, and the excrements from extant snakes cited in this report all come from terrestrial forms. Tortoises and snakes are poor analogs for coprolites that are preserved in fluvial or lacustrine sediments, unless the coprolites are assumed to have been transported. I can see no reason to exclude creatures such as crocodiles or large fish as possible coprolite producers, or mammals equivalent to modern beaver, otter, or muskrat..

<i>Tinca</i> sp.	<i>Palaeotinca</i> sp., <i>Palaeotinca egeriana</i> , <i>Palaeotinca obtruncata</i>
------------------	---

262

263 **Table 4.** List of taxa of observed amphibian excrements. Fossil representatives taken from
264 Hunt & Lucas, 2007.

265

modern amphibians	fossil representative
<i>Andrias</i> sp.	<i>Andrias bohemicus</i> , <i>Andrias</i> cf. <i>scheuchzeri</i> , <i>Chelotriton</i> cf. <i>paradoxus</i>

266

267 **Table 5.** List of taxa of observed bird excrements. Fossil representatives taken from Hunt &
268 Lucas, 2007.

269

modern birds	fossil representative
<i>Phalacrocorax</i> sp.	<i>Nectornis</i> sp., <i>Phalacrocorax littoraris</i>
Strigiformes indet.	<i>Prosybris antiqua</i> , <i>Mioglaux debellatrix</i> , <i>Intulula tinnipara</i>
<i>Aquila</i> sp.	<i>Polemaetus</i> sp.
<i>Accipiter</i> sp.	Accipitridae indet.

270

271 **Table 6.** List of taxa of observed mammals excrements. Fossil representatives taken from
272 Hunt & Lucas, 2007.

273

modern mammals	fossil representative
<i>Ursus</i> sp.	<i>Ursavus elmensis</i> , <i>Ursavus isorei</i> , <i>Tomocyon</i> sp., <i>Hemicyon</i> cf. <i>stehlini</i> , <i>Amphicyon bohemicus</i> , <i>Amphicyon major</i> , <i>Megamphicyon giganteus</i> , <i>Cynelos schlosseri</i>
Rhinocerotidae indet.	<i>Mesaceratherium</i> aff. <i>paulhiacense</i> , <i>Prosantorhinus laubei</i> , <i>Protaceratherium minutum</i>

<i>Cervussp.</i>	<i>Procervulus cf. praelucidus</i>
Equidae indet.	<i>Anchitherium aurelianense</i>

Results

“Coprolite” morphotypes

29 specimens of excrement-shaped ferruginous masses were collected. Among these specimens two different shapes and sizes were identified. More specifically, morphotype 1 (M1) is represented by small (up to 40 mm long, see Table 7) sausage-shaped specimens with smooth or rough surface and flared lower part (Fig. 2A, B). Morphotype 2 (M2), in turn, is represented by large (up to 63 mm long) and more rounded to oval, massive specimens with rough surface (Fig. 2E-G). Rare specimens (Fig. 2F, G) included into M2, bear prominent pointed end covered by striate pattern (herein interpreted as a trace produced after closing anus, see Discussion below). Color of both morphotypes varies from pale orange, through greenish red, to burgundy-colored.

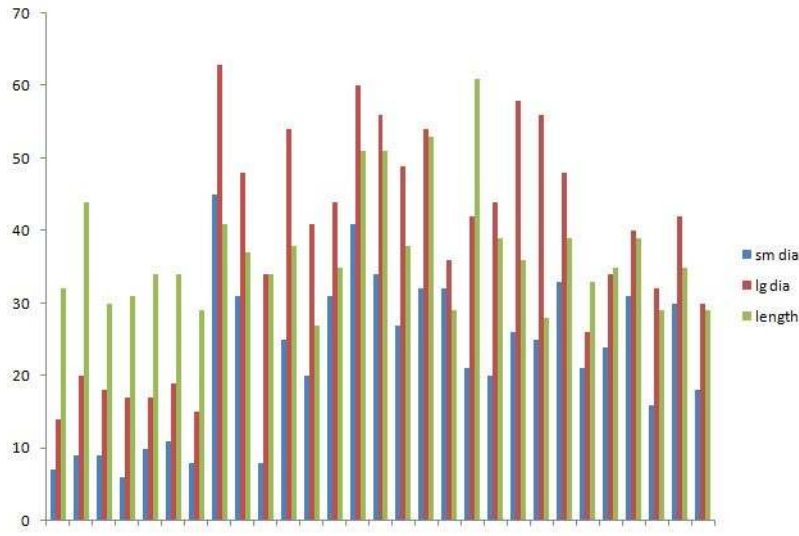


Figure 2 around here

Table 7. Summary for excrement-shaped ferruginous masses.

Comment [GM11]: The morphological characteristics are not well presented in this data table. I suggest that a bar graph would provide more clarity. I am attaching an Excel graph that I made using the data from figure 7. I am including it here as an example, not as an actual addition to the manuscript. The graph shows that the morphotype divisions are rather complex.

Length is a questionable parameter for establishing morphotypes: the text describes M1 lengths as being up to 40mm, but “M1” specimen 2 has a 43mm length. The descriptions of shape (e.g. “more rounded” are not quantifiable, making the morphotype designations rather subjective. Perhaps specimen mass (weight) is a useful parameter. Or volume, which could be measured by hydrostatic displacement.

Comment [GM12]: The morphotype division is an important observation, as is the scarcity of specimens. The situation is very different in the Miocene “coprolites” of the Wilkes Formation of Washington State. Thousands of specimens have been collected, and they are highly varied in size, ranging in length from tiny to very large, I believe this is also true of the Whitemud Formation in Saskatchewan, where a vast number of specimens have been collected from Late Cretaceous clay beds. Broughton (2017) divides the Whitemud specimens into two morphotypes based on shape, noting that lengths can vary from 1-2cm to more than 1m. In both deposits, size alone does not provide a basis for morphotype division.

One of the virtues of this manuscript is that it describes an occurrence of ferruginous “coprolites” that has distinctive differences from deposits like Wilkes Fm. and Whitemud Fm. It supports my belief that there is not a single geologic and paleoenvironmental model that explains all occurrences. It is a reason why this research has scientific importance.

specimen no.	morphotype	dimensions (diameter at its narrowest point*diameter at its widest point*length); all are given in mm	inferred producer
GIUS 10- 3739/1	M1 (see Fig. 2B, C)	7*14*32	Testudinoidea
GIUS 10- 3739/2	M1 (see Fig. 2A)	9*20*44	Testudinoidea
GIUS 10- 3739/3	M1	9*18*30	Testudinoidea
GIUS 10- 3739/4	M1	6*17*31	Testudinoidea
GIUS 10- 3739/5	M1	10*17*34	Testudinoidea
GIUS 10- 3739/6	M1	11*19*34	Testudinoidea
GIUS 10- 3739/7	M1	8*15*29	Testudinoidea
GIUS 10- 3739/8	M2 (see Fig. 2F)	45*63*41	Serpentes
GIUS 10- 3739/9	M2 (see Fig. 2G)	31*48*37	Serpentes
GIUS 10- 3739/10	M2 (see Fig. 2I, J)	8*34*34	Serpentes
GIUS 10- 3739/11	M2 (see Fig. 2K)	25*54*38	Serpentes
GIUS 10- 3739/12	M2 (see Fig. 2M)	20*41*27	Serpentes
GIUS 10- 3739/13	M2	31*44*35	Serpentes
GIUS 10- 3739/14	M2	41*60*51	Serpentes
GIUS 10- 3739/15	M2	34*56*51	Serpentes
GIUS 10- 3739/16	M2	27*49*38	Serpentes
GIUS 10- 3739/17	M2	32*54*53	Serpentes
GIUS 10- 3739/18	M2	32*36*29	Serpentes
GIUS 10- 3739/19	M2	21*42*61	Serpentes
GIUS 10- 3739/20	M2	20*44*39	Serpentes
GIUS 10- 3739/21	M2	26*58*36	Serpentes
GIUS 10- 3739/22	M2	25*56*28	Serpentes
GIUS 10- 3739/23	M2	33*48*39	Serpentes

GIUS 10-3739/24	M2	21*26*33	Serpentes
GIUS 10-3739/25	M2	24*34*35	Serpentes
GIUS 10-3739/26	M2	31*40*39	Serpentes
GIUS 10-3739/27	M2	16*32*29	Serpentes
GIUS 10-3739/28	M2	30*42*35	Serpentes
GIUS 10-3739/29	M2	18*30*29	Serpentes

Thin sections made from specimens no. GIUS 10-3739/28, 29 are acronymed GIUS 10-3739/TS.

Optical microscopy, microtomographic and palaeontological studies

The thin sections from two specimens representing two morphotypes were studied both under transmitted and reflected light optical microscopy. The sections from both morphotypes look very similar. They are dominated by darker matrix almost not translucent making transmitting light observations difficult. The mineral matrix seems to be rather homogenous. Within the matrix of M2-type more translucent elongated straight or curly structures (up to about few mm long and 10-99 µm thick; mean: 52 µm) are visible (Fig. 3). The structures sometimes form arcs or are twisted. In the reflected light, they seem to be areas of light reduction, while surrounding matrix is oxidized. The dark (rusty-colored, brown to almost black), poorly translucent coloring of a matrix suggests iron-rich mineral which form the matrix. Therefore both mineral matrix as well as thin elongated straight to curly structures were studied in-depth under SEM and Raman imaging (see below). No other distinguishable micro remains were noticed in thin sections. However, at the broken surfaces of some specimens of the first morphotype (M1) some tiny coalified debris were occasionally noticed (Fig. 2A, B).

Figure 3 around here

Microtomographical studies of selected specimen (GIUS 10-3739/23; Supplementary Movie 1) did not reveal any internal structures, which could have been eventually interpreted as undigested food remains.

Mineralogical, geochemical and structural analyses

Comment [GM13]: The authors miss an important reference where the mineralogy of ferruginous "coprolites" is discussed in detail, including optical microscopy and SEM:

Yancey, T.E., Mustoe, G.E., Leopold, E.B., and Heizler, M.T. 2013. Mudflow disturbance in latest Miocene forests in Lewis County, Washington. *Palaios*, v. 28, p. 343-350.

XRD analyses of powdered fragments of two specimens from each morphotypes indicated that they both are composed of siderite with small admixture of goethite, and hematite (Fig.4).

Figure 4 around here

The more detailed data on microstructure and elemental composition were collected by utilizing SEM/EDS. We found that the matrix is composed of irregular forms organized in net-system structures (Fig. 5). These forms are bound by thin walls that often consist of several layers (Fig. 5G, H). The chemical analyses showed that the walls consist of iron oxides and the interior is likely filled with iron carbonate. Two types of matrix occurring in both morphotypes (M1 and M2) were distinguished. The first one includes smaller (up to 10 μm in diameter) forms with a broad wall of iron oxides and an empty inner part (Fig. 5A-F). Occasionally, larger forms with carbonate centers (up to 100 μm in diameter) can also be found in the vicinity of the large voids (Fig. 5G). Due to the presence of unfilled forms in the matrix, a distinct porosity pattern can be visible (Fig. 5A1-F1). In this matrix type, within specimen of M2-type straight or curly elongated structures, which were also observed under optical microscopy, can be found (Fig. 3, 5A-F). They can occur as thin (10-99 μm) lines with significantly limited porosity (Fig. 3, 5A-B1, C-F1). In the widest cross sections, some cellular structure is observed (Fig. 3H, 5A-B1), while in the narrowest cross sections (Fig. 5C-F1), characteristic scale-like pattern is observed (Fig. 3F, G, 5C-F1). The second type of matrix consists of larger (up to 30 μm in diameter) forms characterized by thinner walls (Fig. 5I, J). Their center is always filled with iron carbonate, so there is no distinct porosity, as well as no elongated structures to be found.

Figure 5 around here

To extend the observations and elemental analysis based on SEM, Raman spectra were collected. The data obtained from Raman spectroscopy allows to differentiate two iron oxides within the walls (Fig. 6A,B). The spectrum of the first one has bands at 1322, 662, 407, 296, and 227 cm^{-1} (Fig. 6A), which are characteristic for the hematite (Hanesch, 2009). The second mineral forms only very thin (<1 μm) layers in the hematite. The main bands of its spectrum are 684, 553, 397, 299, and 242 cm^{-1} (Fig. 5B), which allow identifying this mineral as goethite. The 1322 cm^{-1} band at the goethite spectrum originated from the admixture of the

hematite. The spectrum of the carbonate mineral contains bands connected to the typical vibrations of the CO₃ group (Fig. 5C), and it can be recognized as siderite.

Figure 6 around here

The Raman spectroscopy was also used to investigate the thin elongated structures in the matrix. There was no variation in the mineralogical composition of these forms in comparison to the matrix. However, during experiments with the 532 nm laser (green), we observed increased fluorescence in the area of the elongated structures with reduced porosity (Fig. 7). This may indicate that although these structures are composed of the same minerals as the matrix, their original chemical composition was different.

Figure 7 around here

Comparative actualistic studies

For comparative purposes we investigated modern faeces (789 in total) produced by a number of vertebrates, comprising all major groups (i.e., fish, amphibians, reptiles, birds, and mammals) (for details see Tables 3-6). We compared our fossil specimens with excrements of extant fish, amphibians, birds and mammals, but they differ in size and shape, and therefore were not subject to further observations. We noticed, however, that our excrement-shaped ferruginous masses ascribed to the morphotype 1 are very similar to sausage-shaped excrements produced by two testudinid turtle taxa [i.e., the Mediterranean tortoise (*Testudo hermanni*) and the steppe tortoise (*Testudo horsfieldii*)]. Their surfaces are mainly smooth and rarely covered with cracks (e.g., Fig. 3C, D); the digested plant debris are sometimes visible on their surfaces (Fig. 3C, D). We also compared these fossil excrements with excrements of other extant turtles [another testudinid, i.e., the Indian star tortoise (*Geochelone elegans*), a geoemydid, i.e., the Spanish pond turtle (*Mauremys leprosa*), and a trionychid, i.e., the Nile softshell turtle (*Trionyx triunguis*)], but the faeces of the *Trionyx triunguis* differ in size and shape. On the other hand, our excrement-shaped ferruginous masses ascribed to the morphotype 2 are very similar to more or less rounded to oval, massive excrements produced by three snake taxa [the king python (*Python regius*), the common boa (*Boa constrictor*), and the king cobra (*Ophiophagus hannah*)]. Their surfaces are rough, and often contain some remnants of etched hair and feathers (e.g., Fig. 3H, I). Moreover, the faeces of the Korean rat

snake (*Elaphe anomala*) are also similar to the fossil morphotype 1; however, they differ in size (they are smaller, cf. Fig. 3L). The excrement surfaces of the latter species are covered by some hairs. We also observed three excrements of the common European viper (*Vipera berus*). They are different in shape and size one from another, their surfaces are covered by etched hair (Fig. 3M).

Discussion

Although in the Biedrzychowice Fm there are numerous inorganic siliceous and siderite concretions (Kasiński et al., 2010; personal observations), they have a different external morphology (i.e., they do not reveal a characteristic excrement-like shape) and internal structure (i.e., they typically have a concentric zoning). On the one hand, results of our geochemical, mineralogical, petrographic and microtomographical analyses indicate that excrement-shaped masses from Poland mainly consist of siderite and iron oxide rather than phosphate, and rarely contain recognizable food residues, which may indicate abiotic origins of these structures. However, evidence in support of a fecal origin include: (i) the presence of two distinct morphotypes differing in size and shape, (ii) the limited quantity of specimens, (iii) the presence of rare fine striations on the surface of some specimens, and (iv) the presence of hair-like elongated structures or coalified inclusions.

Spencer (1993) argued that parallel striations in the pseudocoprolites from the Miocene of southwestern Washington State might have resulted from passage of the material over the grain of the wood. However, fine striations visible on the surface of two specimens from Poland are more reminiscent of marks left by the anal sphincter because they are not randomly distributed but are located in the pointed end of the specimens (Fig. 3F, G). Likewise, they differ from longitudinal parallel striations observed in the specimens ascribed to gut casts of giant terrestrial earthworms (Broughton, 2017).

Although mineralogy of the excrement-shaped masses from Poland is not indicative of coprolites, it might have been a result of diagenesis (Broughton et al., 1977, 1978; Broughton, 2017). Indeed, Seilacher et al. (2001) noted that similar excrement-shaped ferruginous masses from the Miocene of southwestern Washington State might have been alternated by secondary processes referred to as the 'roll-fronts' of oxidized groundwater (Goldhaber et al., 1979; Harris & King, 1993), which dissolves calcite and phosphates bones and precipitates ferroan carbonates. The presence of numerous voids and lack of clay minerals within excrement-shaped ferruginous masses from Poland is consistent with this scenario. Furthermore, lack of

Comment [GM14]: A problem with the roll-front model is that it requires flow of groundwater through the sediment, but ferruginous "coprolites" commonly occur in clay beds that have low permeability. There are many studies of roll-front deposits because of their economic importance for the origin of minerals like uranium or silver (e.g., Silver Reef, Utah). These deposits typically occur in ancient channel deposits that contain coarse clastic sediment with high permeability. Roll front mineralization may involve replacement of organic matter, but this is problematic for ferruginous "coprolites". As an example in the Wilkes Formation of Washington, the "coprolites" occur in strata that contain large amounts of wood. The surrounding clay has so thoroughly protected the wood that it was not subject to decay or mineralization. It is hard to imagine a geochemical process where fecal or intestinal remains would become completely replaced by iron minerals while the adjacent wood remains unaltered. The reference to Seilacher et al. hypothesis of roll-front mineralization perpetuates an unsubstantiated claim. There is a fundamental enigma regarding the origin of these ferruginous extrusions. Paleontologists note the striking excremental form of these objects, but they rarely report detailed stratigraphic and taphonomic characteristics, or geochemical processes that could have produced the mineralization.

Comment [GM15]: Seilacher based his observations on some specimens that had been purchased at a mineral fair in Connecticut. He never visited the site, and had little if any knowledge of the geologic setting. Broughton (2021) asserts that the iron mineralization was a result of microbial biofilms that resulted in precipitation of ferrihydrite/goethite, and that siderite is a diagenetic alteration product, not a primary precipitate. I am not supporting this hypothesis, but it is a topic that deserves mention in the geologic overview:

Reference: Broughton, P.A. 2021. Ferruginous casts in kaolin beds: microbial ferrihydrite-goethite transformation as early stage taphonomy in lacustrine and riparian sediments: Lethaia. This is available online at DOI 10.1111/let.12455

phosphates in the coprolites may be additionally explained by the fact they were produced by predominantly herbivorous animals (Chin & Kirkland, 1998; Fiorelli et al., 2013; Bajdek et al., 2016). Notably, within the morphotype 1 some tiny coalified debris were noted. The morphotype 2, in turn, contains only some elongated thin structures. They are reminiscent of hairs. Their mean size (52 μm) falls well within the range of the hair diameter (4-160 μm) of extant animals (Mayer, 1952; Schneider & Buramuge, 2006; Kshirsagar et al., 2009). Furthermore, their morphologies, i.e., some cellular structure observed in the widest longitudinal sections (Fig. 2H, 5A-B1) and characteristic scale-like pattern observed in the narrowest longitudinal sections (Fig. 5C-F1), are similar to the inner cellular structure of medulla (wide medulla lattice type *sensu* Schneider & Buramuge, 2006, fig. 2) and outer scale-like layers (regular wave pattern *sensu* Schneider & Buramuge, 2006, fig. 4) of the extant and fossil hairs (e.g., fig. 2b, d in Meng & Wyss, 1997; figs. 3-9 in Taru & Backwell, 2013). If these excrement-shaped masses indeed represent true coprolites, this may indicate that the digestive system of the producer was highly efficient, i.e., it dissolved and absorbed everything but the prey's hair, which were excreted along with faeces.

The presence of two distinct morphotypes, differing in size and shape suggests that they might have been expelled from the two different producers. Indeed, comparative actualistic study of Recent vertebrate faeces show overall resemblance of the first morphotype (sausage-shaped with rare coalified debris) to excrements of turtles of the group Testudinoidea. This is further supported by the fact that a testudinoid shell fragment was also recovered in the Turów mine, that being also the sole so far found vertebrate fossil from that locality. Within Testudinoidea, tortoises (Testudinidae) are terrestrial, while the other two groups that inhabited and still inhabit Europe (Emydidae and Geoemydidae) are aquatic or at least semiaquatic – as such, it seems most probable that the Polish excrements were produced by a terrestrial testudinid. Testudinoids have been already known in the Polish fossil record, however, their earliest occurrence so far was documented in younger strata, i.e., the middle Miocene (MN 6) locality of Nowa Wieś Królewska near Opole (Wegner, 1913). That being said, the single shell fragment from Turów represents the earliest testudinoid occurrence from Poland. Nevertheless, testudinoids are already known from early Miocene localities in the vicinity area of northwestern Czech Republic and southeastern Germany (see Table 2). Other turtle lineages, such as chelydrids and trionychids are found in the same vicinity area – among them, the former group is also found in the middle Miocene of Poland (Joyce, 2016), while the latter has never been so far identified from that country (Georgalis & Joyce, 2017). On the other hand, the second coprolite morphotype from the Turów mine (morphotype M2)

approaches more in its overall morphology the excrements of extant species of snakes. More particularly, there is a high degree of resemblance with large snake species of *Constrictores* (*sensu* Georgalis & Smith, 2020; i.e., booids and pythonoids). Nevertheless, an overall resemblance of M2 is also apparent with excrements of large caenophidians, such as the elapid *Ophiophagus* and the colubrid *Elaphe*, while, conversely, smaller caenophidian taxa, such as the viperid *Vipera berus* and the colubrid *Pantherophis*, seem to produce very differently-shaped excrements, which are relatively thin and tightly curled. As such, it is probable that the excrement shape within snake taxa could be somehow size-constrained and does not have a clear taxonomic/phylogenetic value as per its exact affinities. In addition, lizards can be excluded as possible candidate producers for morphotype M2, as excrements of extant large lizard taxa, such as anguids and varanids (which have also an abundant fossil record in the early Miocene of Central Europe) were much differently-shaped. This being said, on the absence of any accompanying skeletal fossil specimen from Turów, we can only infer that the coprolite morphotype M2 was produced by large, but still indeterminate, snakes. Afterall, large snakes were rather abundant in the Burdigalian of Central Europe, being also rather diverse, pertaining to a number of different lineages (Booidea, Pythonoidea, Colubridae, Natricidae, Elapidae, Viperidae) (see Table 2). It is noteworthy that snakes are known to maintain of a very acidic pH during digestion and dissolve and absorb everything but the prey's hair (or feathers) and claws, which are excreted along with waste (Pope et al., 2007; Nørgaard et al., 2016).

475

476 **Conclusions**

477

The excrement-shaped ferruginous masses and the turtle shell fragment from the early Miocene of Turów mine in Poland have been described for the first time. Although different hypotheses were invoked to explain the origins of similar excrement-shaped ferruginous masses, we favour the hypothesis that at least the specimens from Poland represent true coprolites. Evidence in support of a fecal origin of these structures include: (i) the presence of two distinct morphotypes differing in size and shape, (ii) the limited quantity of specimens, (iii) the presence of hair-like structures or coalified inclusions and (iv) the presence of rare fine striations on the surface. If zoological in origin, the first morphotype (sausage-shaped with rare coalified debris) might have been produced by tortoises (Testudinoidea), whereas the second morphotype (rounded to oval-shaped with hair-like structures) might represent fossil faeces of snakes (Serpentes).

489

490 **Acknowledgements**

491

492 We are particularly grateful to Marek Mitrenga, Director of the Silesian Zoological Garden,
493 for making it possible for us to observe the faeces of modern reptiles. Andrzej Malec and
494 Adriana Strzelczyk from the Silesian Zoological Garden provided help, logistic support and
495 information on the mode of life and diet of reptiles kept in the Silesian Zoological Garden.
496 We would also like to thank the dozens of breeders from Poland and the Czech Republic for
497 acquiring modern research material. Our thanks are also due to the management of the Turów
498 Brown Coal Mine for granting permission to enter the plant, and in particular to Ewa
499 Dąbrowska, who supported us with advice and provided all logistical assistance during the
500 field works. Eligiusz Szeleg is acknowledged for providing an access to Olympus BX51
501 polarizing microscope. This research Project is partially supported by the National Science
502 Centre, Poland (www.ncn.gov.pl), Grant No. 2019/32/C/NZ4/00150. GLG acknowledges
503 funding from Forschungskredit of the University of Zurich, Grant no. [FK-20-110].

504

505 **References**

- 506 **Amstutz G. 1958.** Coprolites: A review of the literature and a study of specimens from
507 southern Washington. *Journal of Sedimentary Petrology* **28**:498–508.
- 508 **Bajdek P, Qvarnström M, Owocki K, Sulej T, Sennikov AG, Golubev VK, Niedźwiedzki**
509 **G. 2016.** Microbiota and food residues including possible evidence of pre-mammalian
510 hair in Upper Permian coprolites from Russia. *Lethaia* **49**:455–477.
- 511 **Bellon H, Bužek C, Gaudant J, Kvaček Z, Walther H. 1998.** The České Středohoří
512 magmatic complex in Northern Bohemia 40K–40Ar ages for volcanism
513 and biostratigraphy of the Cenozoic freshwater formations. *Newsletters on Stratigraphy*
514 **36**:77–103.
- 515 **Böhme M. 1996.** *Revision der oligozänen und unter-miozänen Vertreter der Gattung*
516 *Palaeoleuciscus (Teleostei, Cyprinidae) Mitteleuropas*. University Leipzig.
- 517 **Böhme M. 1998.** *Archaeotriton basalticus* (v. Meyer, 1859) (Urodela, Salamandridae) aus
518 dem Unteroligozän von Hammerunterwiesenthal (Freistaat Sachsen). *Abhandlungen des*
519 *Staatlichen Museums für Mineralogie und Geologie zu Dresden* **43/44**:265–280.
- 520 **Böhme M. 2007.** Revision of the cyprinids from the Early Oligocene of the České Středohoří
521 Mountains, and the phylogenetic relationships of *Protothymallus* Laube 1901

(Teleostei, Cyprinidae, Gobioninae). *Acta Musei Nationalis Pragae, Ser. B, Hist. Nat.* **63**:175–194.

Broughton PL. 2017. Enigmatic origin of massive Late Cretaceous-to-Neogene coprolite-like deposits in North America: a novel palaeobiological alternative to inorganic morphogenesis. *Lethaia* **50**:194–216.

Broughton PL, Simpson F., Whitaker SH. 1977. Late Cretaceous coprolites from southern Saskatchewan: comments on excretion, plasticity and ichnological nomenclature. *Bulletin of Canadian Petroleum Geology* **25**:1097–1099.

Broughton PL, Simpson F., Whitaker SH. 1978. Late Cretaceous coprolites from western Canada. *Palaeontology* **21**:443–453.

Čerňanský A. 2010a. A revision of chamaeleonids from the Lower Miocene of the Czech Republic with description of a new species of *Chamaeleo* (Squamata, Chamaeleonidae). *Geobios* **43**:605–613.

Čerňanský A. 2010b. Earliest world record of green lizards (Lacertilia, Lacertidae) from the Lower Miocene of Central Europe. *Biologia* **65**:737–741.

Čerňanský A. 2012. The oldest known European Neogene girdled lizard fauna (Squamata, Cordylidae), with comments on Early Miocene immigration of African taxa. *Geodiversitas* **34**:837–848.

Čerňanský A, Joniak P. 2009. Nové nálezy jašteríc (Sauria, Lacertidae) z neogénnych sedimentov Slovenska a Českej republiky. *Acta Geologica Slovaca* **1**:57–64.

Čerňanský A, Bauer AM. 2010. *Euleptes gallica* Müller (Squamata: Gekkota: Sphaerodactylidae) from the Lower Miocene of North-West Bohemia, Czech Republic. *Folia Zoologica* **59**:323–328.

Čerňanský A, Augé M. 2012. Additions to the lizard fauna (Squamata: Lacertilia) of the Upper Oligocene (MP 28) of Herrlingen 8, Southern Germany. *Neues Jahrbuch für Geologie und Paläontologie, Abhandlungen* **264/1**:11–19.

Čerňanský A, Augé M. 2013. New species of the genus *Plesiolacerta* (Squamata: Lacertidae) from the upper Oligocene (MP 28) of southern Germany and a revision of the type species *Plesiolacerta lydekkeri*. *Palaeontology* **56**:79–94.

Čerňanský A, Rage J-C, Klembara J. 2015. The Early Miocene squamates of Amöneburg (Germany): the first stages of modern squamates in Europe. *Journal of Systematic Palaeontology* **13**:97–128.

554 **Čerňanský A, Klembara J, Müller J. 2016.** The new rare record of the late Oligocene
555 lizards and amphisbaenians from Germany and its impact on our knowledge of the
556 European terminal Palaeogene. *Palaeobiodiversity and Palaeoenvironments* **96**:559–
557 587.

558 **Chin K, Kirkland JI. 1998.** Probable herbivore coprolites from the Upper Jurassic Mygatt-
559 Moore Quarry, Western Colorado. *Modern Geology* **23**:249–275.

560 **Chroust M, Mazuch M, Luján ÀH. 2019.** New material from the Eocene–Oligocene
561 transition of the NW Bohemia (Czech Republic): an updated fossil record in Central
562 Europe during the Grande Coupure. *Neues Jahrbuch für Geologie und Paläontologie,*
563 *Abhandlungen* **293**:73–82.

564 **Chroust M, Mazuch M, Ivanov M, Ekrt B, Luján ÀH. 2021.** First remains of
565 *Diplocynodon* cf. *ratelii* from the early Miocene sites of Ahníkov (Most Basin, Czech
566 Republic). *Bulletin of Geosciences* **96**:123–138.

567 **Dake HC. 1939.** *Northwest gem trails: Portland, Oregon.* Mineralogist Publishing Company.

568 **Dake HC. 1960.** Washington coprolites again. *Mineralogist* **28**:2–6.

569 **Danner WR. 1968.** Origin of the siderite coprolite-like bodies of the Wilkes Formation, late
570 Miocene, of southwestern Washington. *Canadian Mineralogist* **9**:571.

571 **Danner WR. 1994.** *The pseudocoprolites of Salmon Creek, Washington.* University of British
572 Columbia Department of Geological Sciences Report.

573 **Danner WR. 1997.** *The pseudocoprolites of Salmon Creek, Washington.* British Columbia
574 Paleontological Symposium.

575 **Dentzien-Dias P, Carrillo-Briceño JD, Francischini H, Sánchez R. 2018.** Paleoeological
576 and taphonomical aspects of the Late Miocene vertebrate coprolites (Urumaco
577 Formation) of Venezuela. *Palaeogeography, Palaeoclimatology, Palaeoecology*
578 **490**:590–603.

579 **Durska E. 2008.** A 90 m-thick coal seam in the Lubstów lignite deposit (Central Poland)
580 palynological analysis and sedimentary environment. *Geological Quarterly* **52**:281–
581 290.

582 **Dvořák Z, Mach K, Prokop J, Knor S. 2010.** *Třetihorní fauna severočeské hnědouhelné*
583 *pánve.* Nakladatelství Granit.

584 **Farlow OJ, Chin K, Argast A, Poppy S. 2020.** Coprolites from the Pipe Creek Sinkhole
585 (Late Neogene, Grant County, Indiana, U.S.A.). *Journal of Vertebrate Paleontology*
586 **30**:959–969.

587 **Fejfar O, Kaiser T. 2005.** Insect bone-modification and paleoecology of Oligocene mammal-
588 bearing sites in the Doupov Mountains, Northern Bohemia. *Palaeontologia Electronica*
589 **8**:1–11.

590 **Fiorelli LE, Ezcurra MD, Hechenleitner EM, Argañaraz E, Taborda JRA, Trotteyn MJ,**
591 **Belén von Baczko M, Desojo JB. 2013.** The oldest known communal latrines prove
592 evidence of gregarism in Triassic megaherbivores. *Scientific Reports* **3**:3348.

593 **Gaudant J. 1996.** Rectifications de nomenclature relatives à l'ichthyofaune oligo-miocène
594 dulcaquicoles de Bohême. *Journal of the Czech Geological Society* **41**:91–96.

595 **Gaudant J. 1997.** Cinq nouveaux gisements de Pelobatidae (Amphibiens anoures) dans
596 l'Oligocène d'Europe centrale. *Neues Jahrbuch für Geologie und Paläontologie,*
597 *Monatshefte* **1997**:434–446.

598 **Georgalis GL, Joyce WG. 2017.** A review of the fossil record of Old World turtles of the
599 clade *Pan-Trionychidae*. *Bulletin of the Peabody Museum of Natural History* **58**:115–
600 208.

601 **Georgalis GL, Smith KT. 2020.** Constrictores Oppel, 1811 – the available name for the
602 taxonomic group uniting boas and pythons. *Vertebrate Zoology* **70**:291–304.

603 **Godfrey JS, Smith BJ. 2010.** Shark-bitten vertebrate coprolites from the Miocene of
604 Maryland. *Naturwissenschaften* **97**:461–467.

605 **Goldhaberet MG, Reynolds LR, Rye OR. 1979.** *Relationship of modern groundwater*
606 *chemistry to the origin and reduction of south Texas roll-front uranium deposits.* U.S.
607 Geological Survey Professional Paper.

608 **Hanesch M. 2009.** Raman spectroscopy of iron oxides and (oxy) hydroxides at low laser
609 power and possible applications in environmental magnetic studies. *Geophysical*
610 *Journal International* **177**:941–948.

611 **Hardie JK. 1994.** Dolomite and siliciclastic dikes and sills in marginal-marine Cretaceous
612 coals of central Utah. *U.S. Geological Survey Bulletin* **2087**:1–19.

613 **Harris R, King KJ. 1993.** Geological classification and origin of radioactive mineralization
614 in Wyoming. In: Snoke AW, Steidmann JR, Roberts SM, eds. *Geology of Wyoming.*
615 Geological Survey of Wyoming Memoir. 898-916.

616 **Hunt AP, Lucas SG. 2007.** Cenozoic vertebrate trace fossils of North America: ichnofaunas,
617 ichnofacies and biochronology. *New Mexico Museum of Natural History and Science*
618 *Bulletin* **42**:17–41.

619 **Hunt AP, Lucas SG. 2012.** Classification of vertebrate coprolites and related trace fossils.
620 *New Mexico Museum of Natural History and Science Bulletin* **57**:137–146.

621 **Hunt AP, Lucas SG. 2021.** The ichnology of vertebrate consumption: dentalites, gastroliths
622 and bromalites. *New Mexico Museum of Natural History and Science Bulletin* **87**:1–216.

623 **Hunt AP, Chin K, Lockley, M. 1994.** The palaeobiology of vertebrate coprolites. In:
624 | Donovan S, ed. *The Palaeobiology of Trace Fossils*. John Wiley and Sons: London.
625 221–240.

626 **Hunt AP, Lucas SG, Spielmann JA, 2012.** The bromalite collection at the National Museum
627 of Natural History (Smithsonian Institution), with descriptions of new ichnotaxa and
628 notes on other significant coprolite collections. *New Mexico Museum of Natural History*
629 *and Science Bulletin* **57**:105–114.

630 **Ivanov M. 2002.** The oldest known Miocene snake fauna from Central Europe: Merkur-North
631 locality, Czech Republic. *Acta Palaeontologica Polonica* **47**:513–534.

632 **Jęczyk M, Sztromwasser E. 1998.** Kominowe sydereytowe dajki karbonatytowe w
633 bazaltoidach Kopalni Węgla Brunatnego Turów (Sudety). *Przegląd Geologiczny* **46**:
634 87–94.

635 **Joyce WG. 2016.** A review of the fossil record of turtles of the clade *Pan-Chelydridae*.
636 *Bulletin of the Peabody Museum of Natural History* **57**:21–56.

637 **Karl HV. 2007.** The fossil reptiles (Reptilia: Chelonii, Crocodylia) from the marine early
638 Oligocene of the Weissenhofer Basin (Central Germany: Saxonia). *Studia Geologica*
639 *Salmantica* **43**:25–66.

640 **Kasiński JR. 2000.** *Atlas geologiczny trzeciorzędowej asocjacji brunatnowęglowej w polskiej*
641 *części Niecki Żytawskiej. Skala 1:50 000*. PIG.

642 **Kasiński JR, Wiśniewski J. 2003.** Stanowisko 5. Formacja biedrzychowska. In: Ciężkowski
643 A, Wojewoda J, Żelaźniewicz A, eds. *Sudety Zachodnie od wendu do czwartorzędu*.
644 WIND: Wrocław. 31–33.

645 **Kasiński JR, Badura J, Przybylski B. 2003.** Cenozoic depressions at the northwestern
646 Sudetic Foreland. In: Ciężkowski A, Wojewoda J, Żelaźniewicz A, eds. *Sudety*
647 *Zachodnie od wendu do czwartorzędu*. WIND: Wrocław. 183–196.

648 **Kasiński JR, Badura J, Pańczyk M, Pécskay Z, Saternus A, Słodkowska B, Urbański P.**
649 **2015.** Osady paleogeńskie w polskiej części niecki żytawskiej – nowe światło na
650 problem wieku zapadliska tektonicznego. *Biuletyn Państwowego Instytutu*
651 *Geologicznego* **461**:295–324.

652 **Kasiński JR, Piwocki M, Swadowska E, Ziemińska-Tworzydło M. 2010.** Lignite of the
653 Polish Lowlands Miocene: Characteristics on a base of selected profiles. *Biuletyn*
654 *Państwowego Instytutu Geologicznego* **439**:99–154.

655 **Klembara J. 1979.** Neue Funde der Gattungen *Ophisaurus* und *Anguis* (Squamata, Reptilia)
656 aus dem Untermiozan Westbohmens (CSSR). *Vestník Ustředního ústavu geologického*
657 **54**:163–169.

658 **Klembara J. 1981.** Beitrag zur Kenntnis der Subfamilie Anguinae (Reptilia, Anguidae). *Acta*
659 *Universitatis Carolinae, Geologica* **2**:121–168.

660 **Klembara J. 2008.** A new anguimorph lizard from the Lower Miocene of North-West
661 Bohemia, Czech Republic. *Palaeontology* **51**:81–94.

662 **Klembara J. 2012.** A new species of *Pseudopus* (Squamata, Anguidae) from the early
663 Miocene of Northwest Bohemia (Czech Republic). *Journal of Vertebrate Paleontology*
664 **32**:854–866.

665 **Klembara, J. 2015.** New finds of anguines (Squamata, Anguidae) from the Early Miocene of
666 North-West Bohemia (Czech Republic). *Paläontologische Zeitschrift* **89**:171–195.

667 **Klembara J, Rummel M. 2018.** New material of *Ophisaurus*, *Anguis* and *Pseudopus*
668 (Squamata, Anguidae, Anguinae) from the Miocene of the Czech Republic and
669 Germany and systematic revision and palaeobiogeography of the Cenozoic Anguinae.
670 *Geological Magazine* **155**:20–44.

671 **Kshirsagar SV, Singh B, Fulari SP. 2009.** Comparative study of human and animal hair in
672 relation with diameter and medullary index. *Indian Journal of Forensic Medicine and*
673 *Pathology* **2**:105–108.

674 **Kvaček Z, Walther H. 2003.** Reconstruction of vegetation and landscape development
675 during volcanic activity in the České Středohoří Mountains. *Geolines* **15**:60–64.

676 **Laube GC. 1901.** Synopsis der Wirbelthier fauna der Böhm. Braunkohlenformation.
677 *Abhandlungen des deutschen naturwissenschaftlich-medizinischen Vereines für*
678 *Böhmen "Lotos"* **2**:107–186.

679 **Love JD, Boyd DW. 1991.** Pseudocoprolites in the Mowry Shale (Upper Cretaceous),
680 northwest Wyoming. *University of Wyoming Contribution to Geology* **28**:139–144.

681 **Major D. 1939.** Origin of Washington „coprolites”. *Mineralogist* **20**:387–389.

682 **Marcinkowski B. 1985.** Przejawy mineralizacji kruszcowej w kompleksie magmowo-
683 metamorficznym okolic Bogatyni. *Kwartalnik Geologiczny* **29**:551–570.

684 **Mayer WV. 1952.** The hair of California mammals with keys to the dorsal guard hairs of
685 California mammals. *American Midland Naturalist* **48**:480–512.

686 **Meng J, Wyss AR. 1997.** Multituberculate and other mammal hair recovered from
687 Palaeogene excreta. *Nature* **385**:712–714.

688 **Micklich N, Böhme M. 1997.** Wolfsbarsch-Funde (Perciformes, Moronidae) aus den
689 Süßwasser-Diatomen von Kučlín (Böhmen) nebst Anmerkungen zur taxonomischen
690 Stellung von "*Perca*" *lepidota* aus den Süßwasserkalken von Öhningen (Baden).
691 *Paläontologische Zeitschrift* **71**:117–128.

692 **Mikuláš R, Fejfar O, Ulrych J, Žigová A, Kadlecová E, Cajz VA. 2003.** Study of the
693 Dětaň locality (Oligocene, Doupovské hory Mts. Volcanic Complex, Czech Republic):
694 collection of field data and starting points for interpretation. *Geolines* **15**:91–97.

695 **Młynarski M, Roček Z. 1985.** Chelonians (Reptilia, Testudines) from the Lower Miocene
696 locality Dolnice (Bohemia, Czechoslovakia). *Časopis pro mineralogii a geologii* **30**:
697 397–408.

698 **Mustoe GEEG. 2001.** Enigmatic origin of ferruginous "coprolites": Evidence from the
699 Miocene Wilkes Formation, southwestern Washington. *GSA Bulletin* **113**:673–681.

700 **Nørgaard S, Andreassen K, Lind Malte C, Enok S, Wang T. 2016.** Low cost of gastric
701 acid secretion during digestion in ball pythons. *Comparative Biochemistry and*
702 *Physiology Part A: Molecular & Integrative Physiology* **194**:62–66.

703 **Obrhelová N. 1971.** Über einen Serranid (Pisces) aus dem nordböhmischem Süßwassertertiär.
704 *Časopis pro mineralogii a geologii* **16**:371–387.

705 **Obrhelová N, Obrhel J. 1987.** Paläoichthyologie und Paläoökologie des kontinentalen
706 Tertiärs und Quartärs in der ČSSR. *Zeitschrift für geologische Wissenschaften* **15**:709–
707 731.

708 **Paszcza K. 2021.** Nowe znaleziska polskich tektytów z obszaru niecki żytańskiej. *Przegląd*
709 *Geologiczny* **69**:244–247.

710 **Pesquero DM, Salesa JM, Espílez E, Mampel L, Siliceo G, Alcalá L. 2011.** An
711 exceptionally rich hyaena coprolites concentration in the Late Miocene mammal fossil
712 site of La Roma 2 (Teruel, Spain): Taphonomical and palaeoenvironmental inferences.
713 *Palaeogeography, Palaeoclimatology, Palaeoecology* **311**:30–37.

714 **Pesquero DM, Souza-Egipsy V, Alcalá L, Ascaso C, Fernández-Jalvo Y. 2014.** Calcium
715 phosphate preservation of faecal bacterial negative moulds in hyaena coprolites. *Acta*
716 *Palaeontologica Polonica* **59**:997–1005.

717 **Piątkowska A, Kasiński J, Graniczny M. 2000.** Analysis of integrated remote sensing and
718 tectonic data in the Żytawa-Zgorzelec Depression (SW Poland). *Przegląd Geologiczny*
719 **48**:991–999.

720 **Pope R, Helmstetter C, Lignot JH, Secor S. 2007.** Bone absorption
721 through specialised intestinal cells in juvenile Burmese pythons. *Comparative*
722 *Biochemistry and Physiology* **146A**:S174.

723 **Reinach A von. 1900.** Schildkrötenreste im Mainzer Tertiärbecken und in benachbarten
724 ungefähr gleichaltrigen. *Abhandlungen der Senckenbergischen Naturforschenden*
725 *Gesellschaft* **28**:1–135.

726 **Roberts AE. 1958.** *Geology and coal resources of the Toledo-Castle Rock District, Cowlitz*
727 *and Lewis Counties, Washington*. U.S. Geological Survey Bulletin.

728 **Roček Z. 1984.** Lizards (Reptilia, Sauria) from the lower Miocene locality Dolnice (Bohemia,
729 Czechoslovakia). *Rozprawy Československé Akademie Ved, Rada Matematických a*
730 *přírodních Ved* **94**:3–69.

731 **Sadowska A. 1995.** Palynostratigraphy and paleoecology Neogene of the Sudetic Foreland.
732 *Annales Societatis Geologorum Poloniae, Wydanie Specjalne* **33**:37–47.

733 **Schneider MF, Buramuge VA. 2006.** Atlas of the Microscopic Hair Structure of Southern
734 African Shrews, Hedgehogs, Golden Moles and Elephant-shrews (Mammalia). *Bonner*
735 *zoologische Beiträge* **54**, 103–172.

736 **Seilacher A, Marshall C, Skinner WC, Tsuihiji T. 2001.** A fresh look at sideritic
737 “coprolites”. *Paleobiology* **27**:7–13.

738 **Spencer PK, Tuttle FH. 1980.** Coprolites or pseudo-coprolites? New evidence concerning
739 the origin of Washington coprolites. *Geological Society of America* **12**:153.

740 **Spencer PK. 1993.** The „coprolites” that arent: The straight poop on specimens from the
741 Miocene of southwestern Washington State, Ichnos. *An International Journal for Plant*
742 *and Animal Traces* **2**:231–236.

743 **Spencer PK. 1997.** The method of multiple working hypotheses in undergraduate education
744 with an example of its application and misapplication. *Journal of Geoscience Education*
745 **45**:123–128.

746 **Špínar ZV. 1972.** *Tertiary frogs from Central Europe*. Academy of Science.

747 **Szyndlar Z. 1991a.** A review of Neogene and Quaternary snakes of Central and Eastern
748 Europe. Part I: Scolecophidia, Boidae, Colubrinae. *Estudios Geológicos* **47**:103–126.

749 **Szyndlar Z. 1991b.** A review of Neogene and Quaternary snakes of Central and Eastern
750 Europe. Part II: Natricinae, Elapidae, Viperidae. *Estudios Geológicos* **47**:237–266.

751 **Szyndlar Z. 1994.** Oligocene snakes of southern Germany. *Journal of Vertebrate*
752 *Paleontology* **14**:24–37.

753 **Szyndlar Z, Schleich H-H. 1993.** Description of Miocene snakes from Petersbuch 2 with
754 comments on the lower and middle Miocene ophidian faunas of southern Germany.
755 *Stuttgarter Beiträge zur Naturkunde B* **192**:1–47.

756 **Szyndlar Z, Rage J-C. 2003.** *Non-erycine Booidea from the Oligocene and Miocene of*
757 *Europe*. Institute of Systematics and Evolution of Animals, Polish Academy of
758 Sciences.

759 **Taru P, Backwell L. 2013.** Identification of fossil hairs in Parahyaena brunnea coprolites
760 from Middle Pleistocene deposits at Gladysvale cave, South Africa. *Journal of*
761 *Archaeological Science* **40**:3674–3685.

762 **Tomassini LR, Montalvo IC, Bargo MS, Vizcaíno FS, Cuitiño IJ. 2019.** Sparassodonta
763 (Metatheria) coprolites from the early-mid Miocene (Santacrucian age) of Patagonia
764 (Argentina) with evidence of exploitation by coprophagous insects. *Palaaios* **34**:639–
765 651.

766 **Wegner RN. 1913.** Tertiär und umgelagerte Kreide bei Oppeln (Oberschlesien).
767 *Palaeontographica* **60**:3–4.

768

769 **Captions to figures and movie:**

770

771 **Fig. 1. A.** Map of central Europe with mentioned in the text areas marked as red rectangles.
772 **B.** Geology of Zittau Basin. **C.** Synthetic lithostratigraphic section of Paleogene and Neogene
773 sediments of the Polish part of the Zittau Basin (slightly modified after Paszcza, 2021).
774

775 **Fig. 2.** Miocene turtle and snake coprolites from the Turów lignite mine, Poland (**A, B, E-G**),
776 compared with modern turtle and snake excrements (**C, D, H-M**) and fossil remain from the
777 Turów lignite mine, Poland (**N**). Scale bar equals 10 mm. **A, B.** coprolites, morphotype M1.
778 **C, D.** modern excrements of *Testudo horsfieldii* (**C**), and *Testudo hermanni* (**D**). **E-G.**
779 coprolites, morphotype M2. **H, I.** modern excrements of *Python regius*. **J.** modern excrement
780 of *Boa constrictor*. **K.** modern excrement of *Ophiophagus hannah*. **L.** modern excrement of
781 *Elaphe anomala*. **M.** modern excrement of *Vipera berus*. **N.** Shell fragment of Testudinoidea
782 indet. from the Turów lignite mine, Poland (**N**).
783 Red arrows in A and B = coalified inclusions, yellow arrows in F and G = fine striations.

784
785
786
787
788
789
790
791
792
793
794
795
796
797
798
799
800
801
802
803
804
805
806
807
808
809
810
811
812

Fig. 3. Hair-like structure identified in coprolites (morphotype 2). A-C. Optical microscopy. D-H. SEM images. F, G. Magnification of scale-like pattern. H. Magnification of internal hair-like cellular structure.

Fig. 4. XRD diffractograms for two coprolite morphotypes. Green line – morphotype 1, red line – morphotype 2.

Fig. 5. (A-F) BSE image of the coprolite matrix with preserved structures. The red frame indicates the area of the Raman image from Fig. 5. **(A1-F1)** topographic pictures of the area from the A-F images. **(G,H)** BSE image of multi-layered iron oxides form with siderite center. **(I,J)** BSE image of the non-porous type of coprolite matrix. Mineral abbreviations: Gth - goethite, Hem - hematite, Sd - siderite.

Fig. 6. Raman spectrum of **(A)** hematite, **(B)** goethite, **(C)** siderite from coprolite matrix.

Fig. 7. The difference in the fluorescence level in the Raman spectrum of hematite from the structures. **(A)** Reflected light image of the elongated structure. **(B)** Cluster analysis of the structure and matrix Raman mapping. **(C)** Raman spectrum of hematite from structure area (1) and coprolite matrix (2).

Supplementary Movie 1. Tomographic animation of Miocene coprolite from Turów.